Optical and scintillation properties of Nd-doped SrAl$_2$O$_4$ crystals

Daisuke Nakauchi[1,*], Go Okada[1], Masanori Koshimizu[2], Takayuki Yanagida[1]

(1. Graduate School of Materials Science, Nara Institute of Science and Technology (NAIST) 8916-5 Takayama-cho, Ikoma-shi, Nara 630-0192, Japan; 2. Department of Applied Chemistry, Graduate School of Engineering, Tohoku University 6-6-07 Aoba, Aramaki, Aoba-ku, Sendai 980-8579, Japan)

Abstract: Nd-doped SrAl$_2$O$_4$ (Nd:SrAl$_2$O$_4$) crystals were prepared by a floating zone (FZ) method with different dopant concentrations. The photoluminescence (PL) measurements under visible light excitations confirmed strong near infrared (NIR) emissions around 890 nm, which is due to the 4f-4f transitions of Nd^{3+}, and the decay time constants were 300–400 μs. Furthermore, VUV excitations revealed two broad emissions around 250–450 and 500–700 nm, which were attributed to self-trapped excitons (STEs) perturbed by Nd^{3+}. Moreover, the X-ray induced scintillation spectra showed some small peaks at around 380 nm in addition to NIR emissions at 1064 nm similarly seen in PL. The former scintillation decay time constants were 30–40 μs. In the undoped sample, these emissions mentioned above were not present but a weak broad emission around 450 nm appeared. In thermally stimulated luminescence (TSL) after X-ray irradiation, strong TSL glow peaks were observed in the Nd-doped samples at around 100 and 250 ℃.

Keywords: scintillation; photoluminescence; storage luminescence; single crystal; rare earths

Inorganic scintillators convert ionizing radiation to thousands of low energy photons (1–6 eV) immediately, so they have been playing an important role in various fields of radiation detections including medical imaging[1], security[2], astrophysics[3], and geophysical and resources exploration, e.g. oil-dwelling[4]. In these applications, market volumes of medical and security fields are especially large, so scintillators for particular X-ray and γ-ray detectors have been intensively studied. A conventional scintillation detector consists of a scintillator, which emits scintillation photons, and a photodetector, which converts the incident photons to electrons. Generally, visible light emitting scintillators are preferable because the most conventional photodetector, PMT, has a high sensitivity around the blue wavelength. In addition to such a conventional visible emitting scintillator, vacuum ultra violet (VUV), UV and near infrared (NIR) scintillators are also attractive for various applications[5,6]. To achieve such a wavelength functionality, rare-earth ions are generally doped as an emission center in bulk insulator or semiconductor materials.

In this study, we investigated the scintillation properties of Nd-doped SrAl$_2$O$_4$ (Nd:SrAl$_2$O$_4$) crystals. In addition, we evaluated the dosimetric properties in order to comprehensively understand the material system. Rare-earth-doped SrAl$_2$O$_4$ have been widely studied in the fields of phosphorescent phosphors[7], and scintilla-

tion from Eu and Dy doped SrAl$_2$O$_4$ in the nano powder or sintered ceramic forms has also been reported[8–12]. Although most scintillation detectors utilize single crystals mainly due to their high detection efficiency and high optical quality, most reported studies of SrAl$_2$O$_4$ materials are in the powder form. For scintillator uses, a bulk form is particularly important since the interaction probability of ionizing radiations with materials simply depends on the detector volume, so except for some specific detectors, most practical detectors use bulk crystalline scintillators. While Nd-doped materials have been regarded as one of the most popular NIR phosphors in laser systems[13], it is also of our great interest as a new generation NIR emitting scintillator. Nd is known to show NIR emission due to the 4f-4f transitions, which has great transparency to biological tissue[14], so it has a considerable potential for bio-imaging applications[6]. It is worth mentioning here that scintillation detectors are usually classified into photon-counting and integration types as commonly utilized in positron emission tomography (PET) and X-ray computed tomography (X-ray CT), respectively. Unlike photon-counting based detection, the integration type does not strictly require a fast scintillator and lifetime of such typical scintillators is on an order of micro-seconds. Up to now, our group also investigated some Nd-doped materials[15,16], and most of them showed detectable scintillation and some materials

were found to be usable even in the photon-counting mode. As far as we are aware, no studies have been reported for the scintillation properties of Nd-doped $SrAl_2O_4$.

1 Experimental

Nd-doped $SrAl_2O_4$ crystals were synthesized by a floating zone (FZ) method using an FZ furnace (FZD0192, Canon Machinery Inc.). We used $SrCO_3$ (99.99%, 1.0 equiv.), Al_2O_3 (99.999%, 1.0 equiv.) and Nd_2O_3 (99.99%, $x/2$ mol.%, x=0, 0.5, 1.0 and 2.0) powders as raw materials. Hereafter, the molar ratio of Nd ions with respect to the $SrAl_2O_4$ compound are used to identify the samples. Here, the Nd ion is expected to substitute the Sr site. These starting compounds were mixed first, and the mixture was shaped to the cylinder by the hydrostatic pressure. Then the cylinder was sintered at 1500 °C for 6 h. The sintered rod was put into the FZ furnace and the crystal growth was conducted with the pulling rate of 5 mm/h and the rotation rate of 20 r/min. The heat radiation source of the FZ furnace is halogen lamp. The synthesized sample was characterized by the measurements below.

To identify the obtained crystalline phase, powder X-ray diffraction (XRD) pattern was measured with a diffractometer (MiniFlex600, Rigaku) over the 2θ range of 5°–70°. The X-ray source is a conventional X-ray tube with a CuKα target operated at 40 kV and 15 mA. The photoluminescence (PL) and PL excitation (PLE) spectra were measured by using a spectrofluorometer (FP8600, JASCO), and PL quantum yield (QY) were evaluated by using Quantaurus-QY (Hamamatsu Photonics). The PL decay time profile monitoring at 890 nm under 575–625 nm excitation was evaluated by using Quantaurus-τ (Hamamatsu Photonics). The excitation source was a white light source, and the band pass filter (11K0350, OptoSigma) was used to select excitation photons. The decay time was deduced by the single exponential fitting. In addition, the emission spectra under VUV photon excitations were measured at the synchrotron facility (UVSOR). The tested excitation wavelength was from 50 to 200 nm.

As a scintillation property, X-ray induced radioluminescence (RL) spectra were measured by utilizing our original setup[17]. The irradiation source was X-ray generator equipped with a tungsten anode target (XRB80P&N200X4550, Spellman). During the measurements, the X-ray generator was supplied with the voltage of 80 kV and tube current of 2.5 mA. While the sample was irradiated by X-rays, the scintillation emissions from the sample were fed into the spectrometer through a 2 m optical fiber to measure the scintillation spectrum. The spectrometer (Andor DU-420-BU2 CCD for visible and Andor DU492A-1.7 for NIR wavelengths

with Shamrock SR163 monochromator) was cooled down to 188 K by a Peltier module to reduce the thermal noise. Furthermore, we have measured the scintillation decay time and afterglow profiles using a pulsed X-ray source equipped afterglow characterization system[18]. In both PL and scintillation decay time profiles, we fitted the data only in the tail part assuming a single exponential function because we cannot evaluate an instrumental response. Here, the afterglow level (A) is represented by A (%)=$100\times(I_2-I_0)/(I_1-I_0)$, where I_0, I_1 and I_2 denote the averaged signal intensity before the X-ray irradiation, the averaged signal intensity during X-ray irradiation and signal intensity at t=20 ms after the X-ray cut off, respectively. Although the evaluation manners of the afterglow differ in each company, we referred the formula from the manner of NIHON KESSHO KOGAKU CO., LTD. which is one of the famous companies for integrated-type scintillation detectors.

In order to characterize relatively shallow trapping centers, the thermally stimulated luminescence (TSL) glow curves were measured by TL-2000 (Nanogray, Japan) with the heating rate of 1 °C/s over the temperature range from 50 to 490 °C[19]. Except for the TSL, the sample for all the other measurements mentioned above was at room temperature.

2 Results and discussion

The synthesized undoped and Nd:$SrAl_2O_4$ crystals are shown in Fig. 1. The samples doped with 0–1.0 at.% Nd look white and translucent, and the 2.0%Nd-doped sample looks colorless and transparent. Since the 2.0%Nd-doped sample has the strongest NIR absorption due to the 4f-4f transitions of Nd^{3+} where the halogen lamp equipped with the FZ furnace has the peak emission wavelength, the crystal growth was stably performed without much creation of cracks and defects. We broke
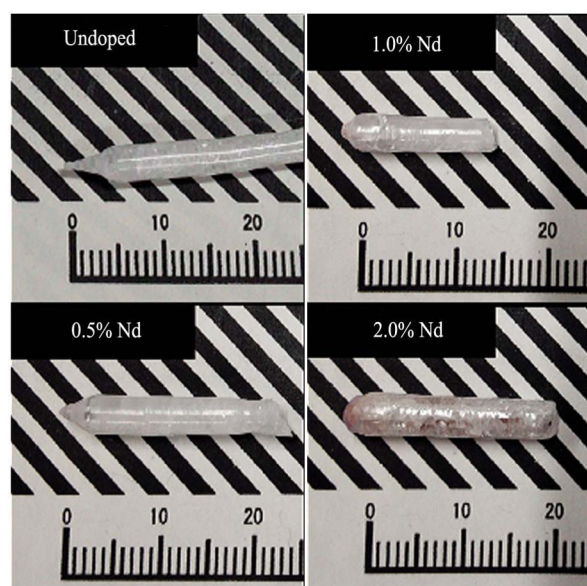

Fig. 1 Appearances of the synthesized Nd:$SrAl_2O_4$ crystals

these crystalline rods to get a few cubic millimeter samples for characterizations.

Fig. 2 shows XRD patterns of the $Nd:SrAl_2O_4$ crystals and the comparison with Crystallography Open Database (COD) information card for 2002284. The XRD patterns are similar for all the samples, and the patterns demonstrate diffraction peaks corresponding to the expected $SrAl_2O_4$ single phase. These materials belong to $P2_1$ space group of the monoclinic crystal system. No impurity phases are observed in whole samples.

The PL and PLE spectra of the 0.5%$Nd:SrAl_2O_4$ crystal are represented in Fig. 3. Some emissions are observed in the 850–950 nm range upon excitations by several different wavelengths. These emissions are due to the 4f-4f transition of Nd^{3+} ($^4F_{3/2} \rightarrow ^4I_{9/2}$)[20]. Under excitation at 585 nm, the QY of the 0.5%, 1.0% and 2.0% $Nd:SrAl_2O_4$ crystals are 29%, 19% and 8.5%, respectively. In the undoped sample, no emissions can be detected. The detection limit of our PL instrument was 1000 nm so we could not observe the most famous Nd^{3+} emission at around 1064 nm.

The PL decay time profiles of the $Nd:SrAl_2O_4$ crystals are represented in Fig. 4. Under an excitation at 575–625 nm
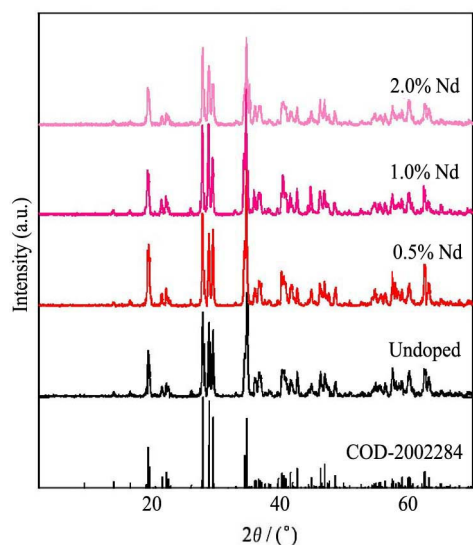

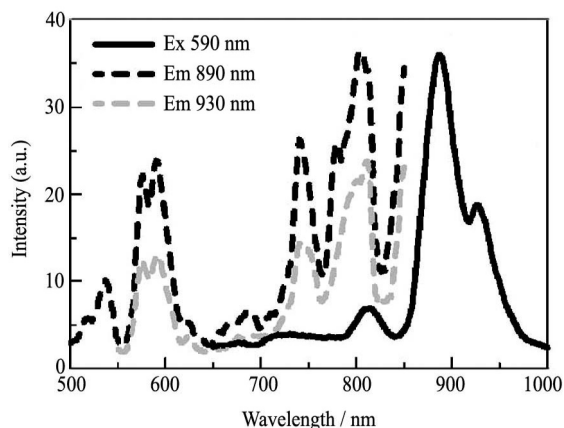Fig. 2 XRD patterns of the $Nd:SrAl_2O_4$ crystals and the comparison with COD information card for 2002284

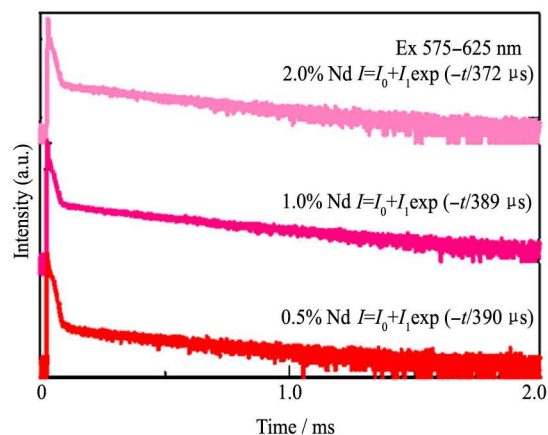Fig. 3 PL and PLE spectra of the 0.5%$Nd:SrAl_2O_4$ crystal

Fig. 4 PL decay time profiles of the $Nd:SrAl_2O_4$ crystals

and monitoring for $^4F_{3/2} \rightarrow ^4I_{9/2}$ (around 900 nm) transition of Nd^{3+}, the PL decay curves are composed of two components. The faster component around the rise part is ascribed to the instrumental response, and the slower component is due to Nd^{3+} emission. The time constants of the 0.5%, 1.0% and 2.0%$Nd:SrAl_2O_4$ crystals are 390, 389 and 372 μs, respectively. These are almost the same as a typical decay time constant of Nd^{3+} [21]. By dense Nd-doping, PL decay time became faster and it was a typical behavior of rare-earth-doped phosphors.

The PL emission spectra of the undoped and 0.5%Nd-doped $SrAl_2O_4$ under VUV photon excitations at UVSOR are represented in Fig. 5. When the Nd-doped sample was excited by 160–180 nm photons, two broad peaks at around 250–450 and 500–700 nm were observed. These peaks cannot be seen in the undoped sample. The band-gap energy of the $SrAl_2O_4$ is reported to be 6.5 eV[22], which corresponds to the energy of a photon with the wavelength of ~190 nm. The excitation wavelength region at which these bands were observed corresponds to the interband excitation. In addition, these bands were not observed with photo-excitation within the band-gap. Hence, electronic transitions within the band-gap at defects or impurities are excluded as the origin. A plausible origin of these bands is self-trapped excitons (STEs) perturbed by Nd^{3+} ions.
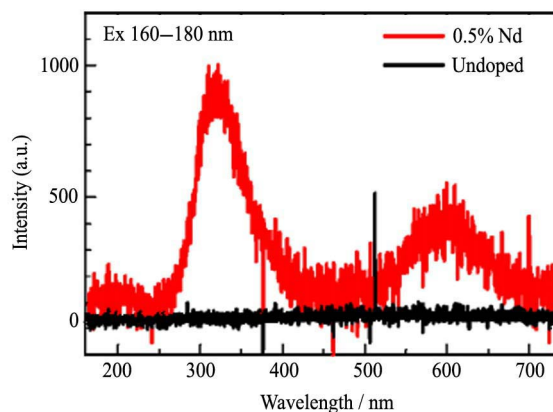

Fig. 5 PL spectra of the undoped and 0.5%Nd-doped $SrAl_2O_4$ crystals under VUV photon excitations
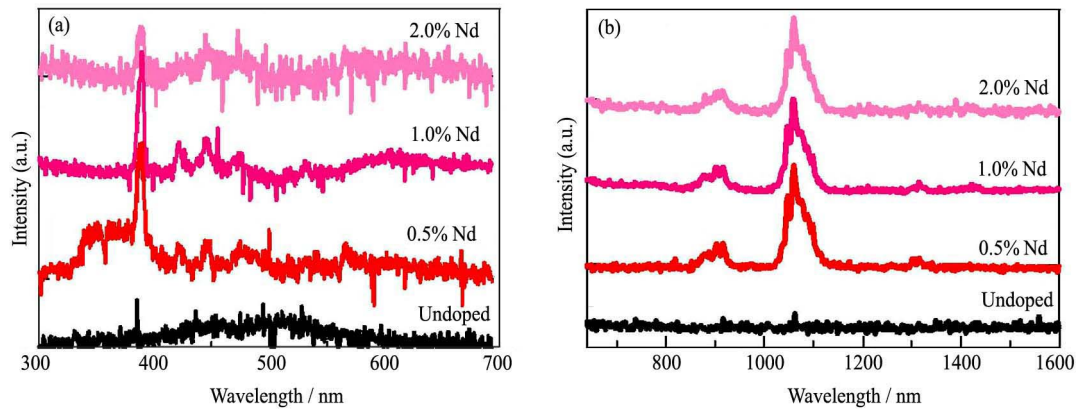
Fig. 6 X-ray induced scintillation spectra of the Nd:SrAl$_2$O$_4$ crystals in UV-Vis (a) and NIR (b) wavelengths

The X-ray induced scintillation spectra are shown in Fig. 6. In UV-Vis range, a sharp emission peak at 380 nm and several emission bands around 450 nm due to 4f-4f transitions of Nd^{3+} (^{2}F(2)$_{5/2}$→^{4}F$_{5/2}$, ^{2}F(2)$_{5/2}$→^{4}F$_{9/2}$, ^{2}F(2)$_{5/2}$→^{4}G$_{5/2}$, ^{2}F(2)$_{5/2}$→^{4}G$_{7/2}$ and ^{2}F(2)$_{5/2}$→^{4}G$_{9/2}$)[23] are observed in Nd-doped samples. Unlike PL, Nd^{3+} emissions in UV-Vis range are detected clearly. In the NIR wavelength, emission peaks are observed at 900, 1064 and 1320 nm. These peaks are attributed to the typical emissions by Nd^{3+} due to the 4f-4f transitions (^{4}F$_{3/2}$→^{4}I$_{9/2}$, ^{4}F$_{3/2}$→^{4}I$_{11/2}$ and ^{4}F$_{3/2}$→^{4}I$_{13/2}$)[15]. In the undoped sample, broad emission bands from 400 to 600 nm is observed. These emission bands were not observed in PL. According to the previous literature[24], the emission around 450 nm was observed only in Eu-doped SrAl$_2$O$_4$ and the origin was interpreted as the charge transfer from the oxygen to residual Eu^{3+}. This scenario is not likely for our sample because our sample does not contain Eu. To consider the origin of these emissions, we also investigated the PL excitation spectrum by using FP8600 (JASCO). The excitation bands monitoring at 450 nm emission appearing was 320 nm. The emission origin was not exciton-related because the excitation energy was smaller than the bandgap, and the origin would be ascribed to some kinds of defects (e.g., oxygen vacancy).

X-ray induced scintillation decay time profiles of the Nd:SrAl$_2$O$_4$ crystals are represented in Fig. 7. The decay
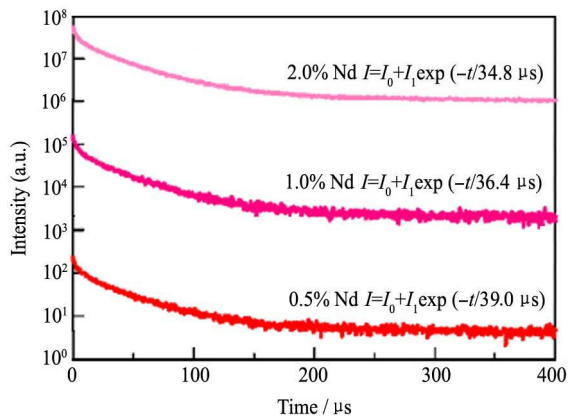
curves consist of one exponential functions, and the time constants of the 0.5%, 1.0% and 2.0%Nd-doped samples are 39.0, 36.4 and 34.8 μs, respectively. As the Nd concentration increase, the decay time become faster. The scintillation decay time is shorter than those in PL due to the difference of the instruments and the evaluation condition. The PMT used in the scintillation evaluation has a wavelength sensitivity from VUV to Vis wavelengths and the sensitivity in NIR wavelength is very low. Therefore main emissions in scintillation decay time profiles are 380–500 nm emission bands, and decay time observed is typical with Nd^{3+} emission in these wavelength ranges[15].

We investigated the afterglow properties after an X-ray irradiation with a pulse duration of 2 ms. The results are shown in Fig. 8. The afterglow levels of the the 0, 0.5%, 1.0% and 2.0% Nd-doped samples are 0.09%, 0.48%, 0.15%, 0.29%, and the 1.0% Nd-doped sample shows the lowest afterglow level among the Nd-doped samples. However, it is much bigger than commercial scintillators such as CdWO$_4$ and BGO (~10 ppm)[18], and these Nd-doped SrAl$_2$O$_4$ are not preferable to high counting rate applications.

The TSL glow curves are shown in Fig. 9. The 1.0%Nd-doped sample shows a TSL glow peak only at lower temperature around 110 ºC, and the 0.5%Nd-
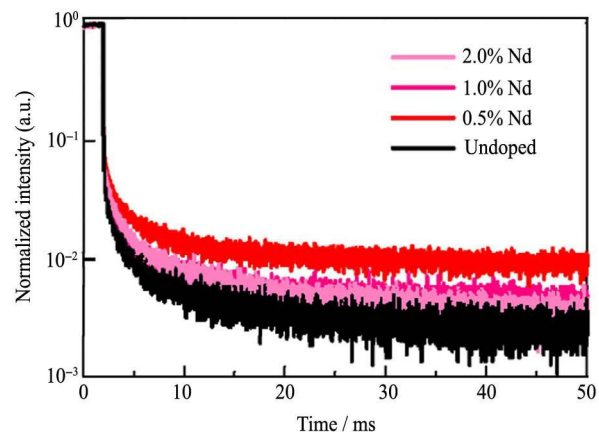

Fig. 7 X-ray induced scintillation decay time profiles of the Nd:SrAl$_2$O$_4$ crystals

Fig. 8 Afterglow curves of the Nd:SrAl$_2$O$_4$ crystals after the X-ray irradiation was cut off
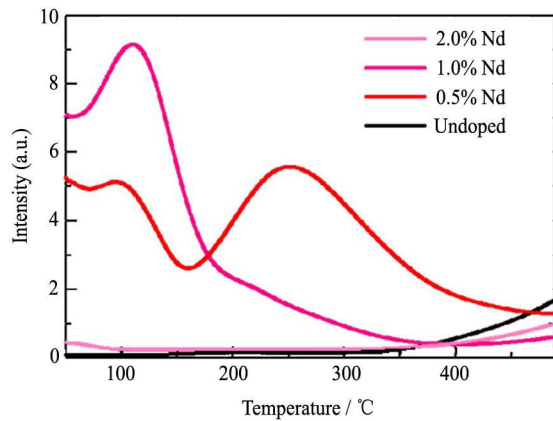
Fig. 9 TSL glow curves of the Nd:SrAl$_2$O$_4$ crystals

doped sample shows a relatively high temperature peak at 250 ºC as well. In the undoped and 2.0%Nd-doped samples, no significant TSL signal is observed. These results are consistent with the afterglow levels since the afterglow is TSL around the room temperature. It is well known that scintillation and PL intensities have a dopant concentration dependence and the optimum doping concentration. If we think analogically with them, TSL may also have an optimum doping concentration, and in this case it was around 1.0%.

3   Conclusions

We investigated the optical, scintillation and dosimetric properties of the Nd:SrAl$_2$O$_4$ crystals synthesized by the FZ method. The Nd:SrAl$_2$O$_4$ crystals showed photo- and radio-luminescence peaks due to the 4f-4f transitions of Nd^{3+} and the decay time constants were almost the same as the typical emissions from Nd^{3+}-doped phosphors. The QY of the 0.5%Nd:SrAl$_2$O$_4$ crystals was the highest among the present samples. Under VUV photon excitations, two broad peaks were observed, and the origins were attributed to STEs perturbed by Nd^{3+} ions. In the afterglow, the undoped sample represented the lowest afterglow level. TSL results suggested that the 0.5%–1.0%Nd-doping concentration was optimum when they worked as the TSL dosimeter.

References:

[1] Yanagida T, Yoshikawa A, Yokota A, Kamada K, Usuki Y, Yamamoto S, Miyake M, Baba M, Sasaki K, Ito M. Development of Pr:LuAG scintillator array and assembly for positron emission mammography. *IEEE. Nucl. Trans. Sci.*, 2010, **57**: 1492.

[2] Totsuka D, Yanagida T, Fukuda K, Kawaguchi N, Fujimoto Y, Yokota Y, Yoshikawa A. Performance test of Si PIN photodiode line scanner for thermal neutron detection. *Nucl. Instrum. Methods A*, 2011, **659**: 399.

[3] Kokubun M, Abe K, Ezoe Y, Fukazawa Y, Hong S, Inoue H, Itoh T, Kamae T, Kasama D, Kawaharada M, Kawano N, Kawashima K, Kawasoe S, Kobayashi Y, Kotoku J, Kouda M, Kubota A, Madejski G M, Makishima K, Mitani T, Miyasaka H, Miyawaki R, Mori K, Mori M, Murakami T, Murashima M M, Nakazawa K, Niko H, Nomachi M, Ohno M, Okada Y, Oonuki K, Sato G, Suzuki M, Takahashi H, Takahashi I, Takahashi T, Tamura K, Tanaka T, Tashiro M, Terada Y, Tominaga S, Watanabe S, Yamaoka K, Yanagida T, Yonetoku D. Improvements of the Astro-E2 hard X-ray detector (HXD-II). *IEEE Trans. Nucl. Sci.*, 2004, **51**: 1991.

[4] Melcher C L. Scintillators for well logging applications. *Nucl. Instrum. Methods B*, 1989, **40/41**: 1214.

[5] Sekiya H, Ida C, Kubo H, Kurosawa S, Miuchi K, Tanimori T, Taniue K, Yoshikawa A, Yanagida T, Yokota Y, Fukuda K, Ishizu S, Kawaguchi N, Suyama T. A new imaging device based on UV scintillators and a large area gas photomultiplier. *Nucl. Instrum. Methods A*, 2011, **633**(1): S36.

[6] Houston J P, Ke S, Wang W, Li C, Sevick-Muraca E M. Quality analysis of *in vivo* near-infrared fluorescence and conventional gamma images acquired using a dual-labeled tumor-targeting probe. *J. Biomed. Opt.*, 2005, **10**: 0540101.

[7] Matsuzawa T, Aoki Y, Takeuchi N, Murayama Y. A new long phosphorescent phosphor with high brightness, SrAl$_2$O$_4$:Eu^{2+},Dy^{3+}. *J. Electrochem. Soc.*, 1996, **143**: 2670.

[8] Montes P J R, Valerio M E G, Azevedo G M. Radioluminescence and X-ray excited optical luminescence of SrAl$_2$O$_4$:Eu nanopowders. *Nucl. Instrum. Methods B*, 2008, **266**: 2923.

[9] Meléndrez R, Arellano-Tánori O, Pedroza-Montero M, Yen W M, Barboza-Flores M. Temperature dependence of persistent luminescence in β-irradiated SrAl$_2$O$_4$:Eu^{2+},Dy^{3+} phosphor. *J. Lumin.*, 2009, **129**: 679.

[10] Montes P J R, Valerio M E G. Radioluminescence properties of rare earths doped SrAl$_2$O$_4$: nanopowders. *J. Lumin.*, 2010, **130**: 1525.

[11] Korthout K, Van den Eeckhout K, Botterman J, Nikitenko S, Poelman D, Smet P F. Luminescence and X-ray absorption measurements of persistent SrAl$_2$O$_4$:Eu,Dy powders: Evidence for valence state changes. *Phys. Rev. B*, 2011, **84**: 085140.

[12] Ayvacıklı M. Ege A, Can N. Radioluminescence of SrAl$_2$O$_4$: Ln^{3+} (Ln=Eu, Sm, Dy) phosphor ceramic. *Opt. Mater.*, 2011, **34**: 138.

[13] Kaminskii A A. Laser Crystals - Their Physics and Properties. Berlin: Springer-Verlag Berlin Heidelberg, 1990.

[14] Jobsis F F. Noninvasive, infrared monitoring of cerebral and myocardial oxygen sufficiency and circulatory parameters. *Science*, 1977, **198**: 1264.

[15] Yanagida T, Sato H. Optical and scintillation properties of Nd-doped complex garnet. *Opt. Mater.*, 2015, **38C**: 174.

[16] Yanagida T, Fujimoto Y, Ishizu S, Fukuda K. Optical and scintillation properties of Nd differently doped YLiF$_4$ from VUV to NIR wavelengths. *Opt. Mater.*, 2015, **41**: 36.

[17] Yanagida T, Kamada K, Fujimoto Y, Yagi H, Yanagitani T. Comparative study of ceramic and single crystal Ce:GAGG scintillator. *Opt. Mater.*, 2013, **35**: 2480.

[18] Yanagida T, Fujimoto Y, Ito T, Uchiyama K, Mori K. De-

velopment of X-ray-induced afterglow characterization system. *Appl. Phys. Exp.*, 2014, **7**: 062401.

[19] Yanagida T, Fujimoto Y, Kawaguchi N, Yanagida S. Dosimeter properties of AlN. *J. Ceram. Soc. Jpn.*, 2013, **121**: 988.

[20] Debieu O, Bréard D, Podhoredecki A, Zatryb G, Misiewicz J, Labbé C, Cardin J, Gourbilleau F. Effect of annealing and Nd concentration on the photoluminescence of Nd^{3+} ions coupled with silicon nanoparticles. *J. Appl. Phys.*, 2010, **108**: 113114.

[21] Merkle L D, Dubinskii M, Schlepler K L, Hedge S M, Concentration quenching in fine-grained ceramic Nd:YAG. *Opt. Exp.*, 2006, **14**: 3893.

[22] Palilla F R, Levine A K, Tomkus M R. Fluorescent proper-
ties of alkaline earth aluminates of the type MAl_2O_4 activated by divalent europium. *J. Electrochem. Soc.*, 1968, **115**: 642.

[23] Sugiyama M, Fujimoto Y, Yanagida T, Yamaji A, Yokota Y. Yoshikawa A. Growth and scintillation properties of Nd-doped $Lu_3Al_5O_{12}$ single crystals by Czochralski and micro-pulling-down methods. *J. Cryst. Growth*, 2013, **362**: 178.

[24] Clabau F, Rocquefelte X, Jobic S, Deniard P, Whangbo M H, Garcia A, Le Mercier T. Mechanism of phosphorescence appropriate for the long-lasting phosphors Eu^{2+}-doped $SrAl_2O_4$ with codopants Dy^{3+} and B^{3+}. *Chem. Mater.*, 2005, **17**: 3904.